Direct Evidence for Epithelial-Mesenchymal Transitions in Breast Cancer

Anthony J. Trimboli,[1,2,3] Koichi Fukino,[2,3] Alain de Bruin,[1,2,3] Guo Wei,[1,2,3] Lei Shen,[4] Stephan M. Tanner,[2,3] Nicholas Creasap,[1,2,3] Thomas J. Rosol,[5] Michael L. Robinson,[6] Charis Eng,[1,2,3,7] Michael C. Ostrowski,[1,2,3] and Gustavo Leone[1,2,3]

[1]Department of Molecular Genetics; [2]Human Cancer Genetics Program, Comprehensive Cancer Center; [3]Department of Molecular Virology, Immunology, and Medical Genetics, College of Medicine; [4]Division of Epidemiology and Biostatistics, School of Public Health; and [5]Department of Veterinary Biosciences, The Ohio State University; [6]Center for Childhood Cancer, Columbus Children's Research Institute, Columbus, Ohio; and [7]Genomic Medicine Institute, Cleveland Clinic Lerner Research Institute and Department of Genetics, Case Western Reserve University School of Medicine, Cleveland, Ohio

Abstract

We developed stromal- and epithelial-specific *cre*-transgenic mice to directly visualize epithelial-mesenchymal transition (EMT) during cancer progression *in vivo*. Using three different oncogene-driven mouse mammary tumor models and cell-fate mapping strategies, we show *in vivo* evidence for the existence of EMT in breast cancer and show that *myc* can specifically elicit this process. Hierarchical cluster analysis of genome-wide loss of heterozygosity reveals that the incidence of EMT in invasive human breast carcinomas is rare, but when it occurs it is associated with the amplification of *MYC*. These data provide the first direct evidence for EMT in breast cancer and suggest that its development is favored by *myc*-initiated events. [Cancer Res 2008;68(3):937–45]

Introduction

The transdifferentiation of epithelial cells to a more mesenchymal state, typically called epithelial-mesenchymal transition (EMT), is an essential process for normal embryonic development that has been implicated in the progression toward an advanced cancer phenotype (1–5). EMT is a multistep process characterized by the loss of cell-to-cell junctions and reorganization of the cytoskeleton, which together result in the loss of apical-basal cell polarity and the acquisition of spindle-shaped morphology (6). This is associated with a decrease in epithelial-specific gene expression, including E-cadherin, and a gain in mesenchymal-specific gene expression. During tumor progression, these changes are thought to ultimately promote tumor cell migration across the basement membrane and invasion into the surrounding microenvironment. EMT in cancer, however, has been inferred predominantly from *in vitro* studies and the expression of cell type–specific markers (7–9). From these studies, epithelial tumor cells that are presumed to undergo EMT acquire a spindle cell morphology that is histologically indistinguishable from normal mammary stromal cells. Because tumor cells *in vivo* have not yet been unambiguously marked and their fate traced during tumor progression, the actual origin of tumor-associated spindle-shaped mesenchymal cells is not known, and hence the occurrence of EMT in cancer remains speculative (10, 11).

Tumor-associated fibroblasts are believed to influence tumor behavior and outcome, and thus understanding their biology is of importance to the overall understanding of cancer. A fundamental premise of EMT in the context of cancer implies that a tumor-associated fibroblast that arises from an EMT event contains a similar set of genetic and/or epigenetic insults as the epithelial tumor cell from which it originated. Because of their genetic differences, fibroblasts that originate from tumor cells would be expected to affect the behavior of cancers differently than fibroblasts that originate from normal mesenchymal progenitors. Whereas results from a large body of work done *in vitro* points to a critical role of EMT in cancer progression, its importance in cancer ultimately rests on whether it actually occurs *in vivo*. The absence of direct evidence for EMT in cancer has therefore raised substantial controversy. To assess the existence of EMT in breast cancer *in vivo*, we developed a genetic system to independently mark epithelial and stromal cells and observe their fate following cancer progression via the expression of *cre* and the $Rosa26^{LoxP}$ reporter allele (12). We also determined genome-wide loss of heterozygosity (LOH) in both epithelial and stromal cells to assess the occurrence of EMT in invasive human breast carcinomas.

Materials and Methods

Generation of *FSP-cre* transgenic mice. The transgene vector for Fsp1-Cre-BGH was created by inserting the BGH polyadenylate signal and the multiple cloning site of pcDNA3 (InvitrogenCA) into a modified pBluescript II plasmid backbone (Stratagene). The 3.1-kb *Fsp1* gene promoter (*S100a4*; refs. 13, 14) extending 1.9 kb upstream of exon 1 to the end of intron 1 (1.2 kb) was long-range PCR amplified (Long Template System) from C57BL/6NTac genomic DNA and cloned into the multiple cloning site of the vector. The Cre recombinase open reading frame from pMC-Cre (15) was PCR amplified and inserted between the *Fsp1* promoter and the BGH polyadenylate signal. Cloning was completed by standard protocols and all fragments were verified by DNA sequencing. All microinjection constructs were injected into pronuclear stage FVB/N mouse embryos, as previously described (16, 17), after the Fsp1-Cre-BGH fragment was excised by *Pac*I (New England Biolabs) digestion and gel purified.

Genotyping of transgenic mice. DNA was isolated from mouse tail tips and genotyped by PCR analysis using the following primer sets (5′ to 3′): *WAP-myc*, CACCGCCTACATCCTGTCCATTCAAGC (forward) and TTAGGACAAGGCTGGTGGGCACTG (reverse), 240 bp; *MMTV-rtTA*, AGTATGCCGCCATTATTACGAC (forward) and CGATGGTAGACCCG-TAATTGTT (reverse), 170 bp; *teto-myc*, GGAATGGCAGAAGGCAGG (forward) and GCAGTAGCCTCATCATCACTAGATGG (reverse), 580 bp;

Note: Supplementary data for this article are available at Cancer Research Online (http://cancerres.aacrjournals.org/).

Requests for reprints: Gustavo Leone, Departments of Molecular Genetics and Molecular Virology, Immunology, and Medical Genetics, Human Cancer Genetics Program, The Ohio State University, 808 Biomedical Research Tower, 460 West 12th Avenue, Columbus, OH 43210. Phone: 614-688-4567; Fax: 614-688-4181; E-mail: gustavo.leone@osumc.edu, or Michael C. Ostrowski, Department of Molecular and Cellular Biochemistry, Human Cancer Genetics Program, The Ohio State University, 810 Biomedical Research Tower, 420 West 12th Avenue, Columbus, OH 43210. Phone: 614-688-3824; Fax: 614-688-4181; E-mail: michael.ostrowski@osumc.edu.

doi:10.1158/0008-5472.CAN-07-2148

MMTV-neu, GGAACCTTACTTCTGTGGTGTGAC (forward) and TAGCAGACACTCTATGCCTGTGTG (reverse), 500 bp; *MMTV-PyMT*, TTCGATCCGATCCTAGATGC (forward) and TGCCGGGAACGTTTTATTAG (reverse), 180 bp; *WAP-cre*, CCAAGAAGGAAGTGTTGTAGCC (forward) and TCCAGGTATGCTCAGAAAACG (reverse), 240 bp; *FSP-cre*, ATGCTTCTGTCCGTTTGCCG (forward) and CAATGCGATGCAATTTCCTC (reverse), 1,082 bp; *teto-cre*, ACTTGCAGTTCTTGCAGGC (common), CCGTAGCTCCAGCTTCACC (wild-type), 588 bp, and CATTTCGTGATGAATGCCAC (cre), 668 bp; *MMTV-cre*, CCTGTTTTGCACGTTCACCG (forward) and ATGCTTCTGTCCGTTTGCCG (reverse), 260 bp; and $Rosa26^{LoxP}$, AAAGTCGCTCTGAGTTGTTAT (common), GCGGGAGAAATGGATAT (wild-type), 550 bp, and GCGAAGAGTTTGTCCTCAACC (transgene), 260 bp.

Mammary tumor models. All animals used for this study were in mixed background of C57BL/6NTac and FVB/NTac, except the MMTV-rtTA/teto-myc/teto-cre model, which was in a 10th generation FVB/N background. Pregnancies for *WAP-myc* and *WAP-cre* induction were started at 8 weeks of age. Females with the *MMTV-neu* and *WAP-myc* oncogenes completed three pregnancies; however, due to the rapid tumor onset in the *MMTV-PyMT* model, *MMTV-PyMT*–positive animals were pregnant only once. Animals were monitored twice a week until tumor onset and sacrificed when the largest tumor was ~2 cm or presented a health problem to the animal, such as exterior ulceration at the site of the tumor. Induction of the MMTV-rtTA/teto-myc system with doxycycline water (2 mg/mL final) was started at 8 weeks of age and continued until animals were sacrificed.

Tissue processing and 5-bromo-4-chloro-3-indolyl-D-galactopyranoside staining. Large individual tumors (typically ~1–2 cm) were excised with portions processed for *in situ* 5-bromo-4-chloro-3-indolyl-D-galactopyranoside (X-gal) staining (below) as well as optimum cutting temperature (OCT) compound embedding (Sakura). Mammary tissue containing small nodes was fixed and stained directly. The lungs and liver were also collected to determine if metastasis had occurred. Tissues were fixed [2% paraformaldehyde/0.2% glutaraldehyde in a 100 mmol/L sodium phosphate buffer (pH 7.4)] for 2 to 2.5 h at 4°C, washed for 10 min twice in 1× PBS, and then stained in an X-gal solution [4 mmol/L potassium ferricyanide (Sigma), 4 mmol/L potassium ferrocyanide (Sigma), 2 mmol/L magnesium chloride (Sigma), 0.2% IGEPAL CA-630 (NP40 substitute; Sigma), 0.1% sodium deoxycholic acid (Calbiochem), and 1 mg/mL X-gal (Gold BioTechnology) in PBS] for 18 h at room temperature protected from light. X-gal–stained tissue was washed for 10 min twice with PBS and postfixed in 10% neutral-buffered formalin (Richard Allen) for 48 h at 4°C. Samples were then paraffin embedded, cut into 5-μm sections, and counterstained with nuclear fast red and H&E. For each X-gal–positive tumor, three sets of sections were obtained at 50-μm intervals for analysis. Corresponding OCT-embedded tissue was sectioned (5 μm) in a similar manner and dried 15 min (room temperature) before fixing [0.2% glutaraldehyde, 1.25 mmol/L EGTA (pH 7.3), 2 mmol/L magnesium chloride in 1× PBS] for 30 min. The sections were washed with LacZ wash buffer [2 mmol/L magnesium chloride, 0.01% sodium deoxycholate, 0.02% IGEPAL CA-630 (Sigma) in PBS] for 5 min thrice and stained in LacZ solution (4 mmol/L potassium ferricyanide, 4 mmol/L potassium ferrocyanide, 1 mg/mL X-gal in LacZ wash buffer) protected from light in a 37°C water bath overnight (~18 h). Sections were washed in PBS for 5 min thrice and then overnight before being rinsed with water for 2 min and counterstained with nuclear fast red. A consecutive section was fixed in 37% formaldehyde for 20 s at room temperature and H&E stained.

Fluorescent immunohistochemistry. All primary and secondary antibodies were diluted in DAKO diluent (DAKO) and applied in the following pairs: goat anti-vimentin (1:50, C-20; Santa Cruz Biotechnology) or goat anti-fibronectin (1:100; Santa Cruz Biotechnology) with donkey anti-goat-Alexa dye conjugate (1:250; Invitrogen/Molecular Probes); guinea pig anti–cytokeratin 8/18 (1:150, RDI-PROGP11; Research Diagnostics) with biotinylated donkey anti–guinea pig (1:500; Jackson Immunochemicals) and streptavidin-Alexa dye conjugate (1:250; Invitrogen/Molecular Probes); and mouse anti–E-cadherin (1:700; BD Biosciences) with donkey anti-mouse-Alexa dye conjugate (1:500; Invitrogen/Molecular Probes). Frozen sections were cut and dried as above, fixed in cold acetone (4°C) for 10 min, and washed in PBS for 10 min. The remaining steps were done at room temperature, rinsing for 1 × 5 min with PBS in between. Sections were blocked with M.O.M. blocking reagent (Vector Labs) for 30 min and rinsed, incubated with primary antibody for 30 min and rinsed, and then incubated with a fluorescently labeled or biotinylated secondary antibody for 15 min and rinsed. Following the biotinylated secondary antibody use, the streptavidin-Alexa dye conjugate was applied for 15 min. The primary/secondary incubations were repeated consecutively for each antibody to achieve double and triple labeling. Sections were washed for 5 min with TBS before incubating with 4′,6-diamidino-2-phenylindole (DAPI; 100 μg/mL in TBS) for 2 min. Sections were washed in TBS followed by a brief rinse in deionized water and coverslipped using Gel/Mount (Biomed).

Images. Photographs of histologic and immunofluorescent sections were taken with an Axio digital camera (Zeiss) mounted on an Axioskop microscope (Zeiss). Whole-mount photographs were taken with a Coolpix 5700 digital camera (Nikon). Image files were processed using Photoshop 7.0 (Adobe) or AxioVision 4.3 software (Zeiss).

Laser capture microdissection from human breast carcinomas. One hundred thirty-one samples originating from 131 women with clinically sporadic, stage I, II, or III invasive breast carcinomas were subjected to laser capture microdissection using the Arcturus PixCell II microscope (Arcturus Engineering, Inc.) to obtain epithelial carcinoma and tumor stromal fibroblasts as previously described (18). Corresponding noncarcinomatous tissue for each carcinoma sample was procured from separate blocks, which were diagnosed by pathologists as containing no carcinomatous tissue (first choice), or, if not possible, from nonneoplastic tissue at a distance from the cancer. In the latter cases, noncarcinomatous tissues were separated from the carcinomatous tissues by normal fat tissue layers. These breast cancer samples were obtained from archived samples in an anonymous fashion, unlinked to patient identifiers as approved by the institutional committee for the protection of human subjects.

Total genome LOH scan. Genomic DNA was extracted as previously described (18, 19) with the exception that incubation in proteinase K was done at 65°C for 2 days. PCR was done using DNA from each compartment of each sample and primer sets, which define 381 microsatellite markers in 72 multiplex panels as recommended by the manufacturer (Research Genetics). Genotyping was done with an ABI 377xl or 3700 semiautomated sequencer (Applied Biosystems, Perkin-Elmer Corp.). The results were analyzed by automated fluorescence detection using the GeneScan collection and analysis software (GeneScan, ABI). Scoring of LOH was done by inspection of the GeneScan output. A ratio of peak heights of alleles between germ-line and somatic DNA ≥1.9:1 was used to define LOH in this study, as with previous studies (20).

Statistical analyses. Informative LOH data from the 262 samples (131 epithelial and 131 stromal derived samples) were used for hierarchical cluster analysis (20). The clustering analysis was based on a dissimilarity matrix, constructed by computing for each pair of samples the frequency of concordance of LOH across all markers that are informative for both samples. Fisher's exact test was used to compare frequencies of allelic imbalance at a given marker between two groups. An imbalance is defined as either amplification or LOH. Therefore, the calculated P value compares the type of allelic imbalance versus the total number of imbalances detected. From five imbalances found in the epithelial samples, all were of amplification type (5 of 5 or 100%). Among the 42 imbalances found in the remaining 117 samples, only 20 were of the amplification type (20 of 42 or 48%). Thus, when we used the Fisher exact test to compare 5 of 5 versus 20 of 42, it resulted in $P = 0.05$.

Results

Generation of a genetic system to mark mammary epithelial and stromal cells *in vivo*. To assess the existence of EMT in breast cancer *in vivo*, we used the $Rosa26^{LoxP}$ reporter mouse to genetically mark tumor epithelial and stromal cells independently and determine their fate during tumor progression. The conditional $Rosa26^{LoxP}$ reporter locus contains a "floxed stop cassette" located in front of the *LacZ* gene. Cre-mediated deletion of the

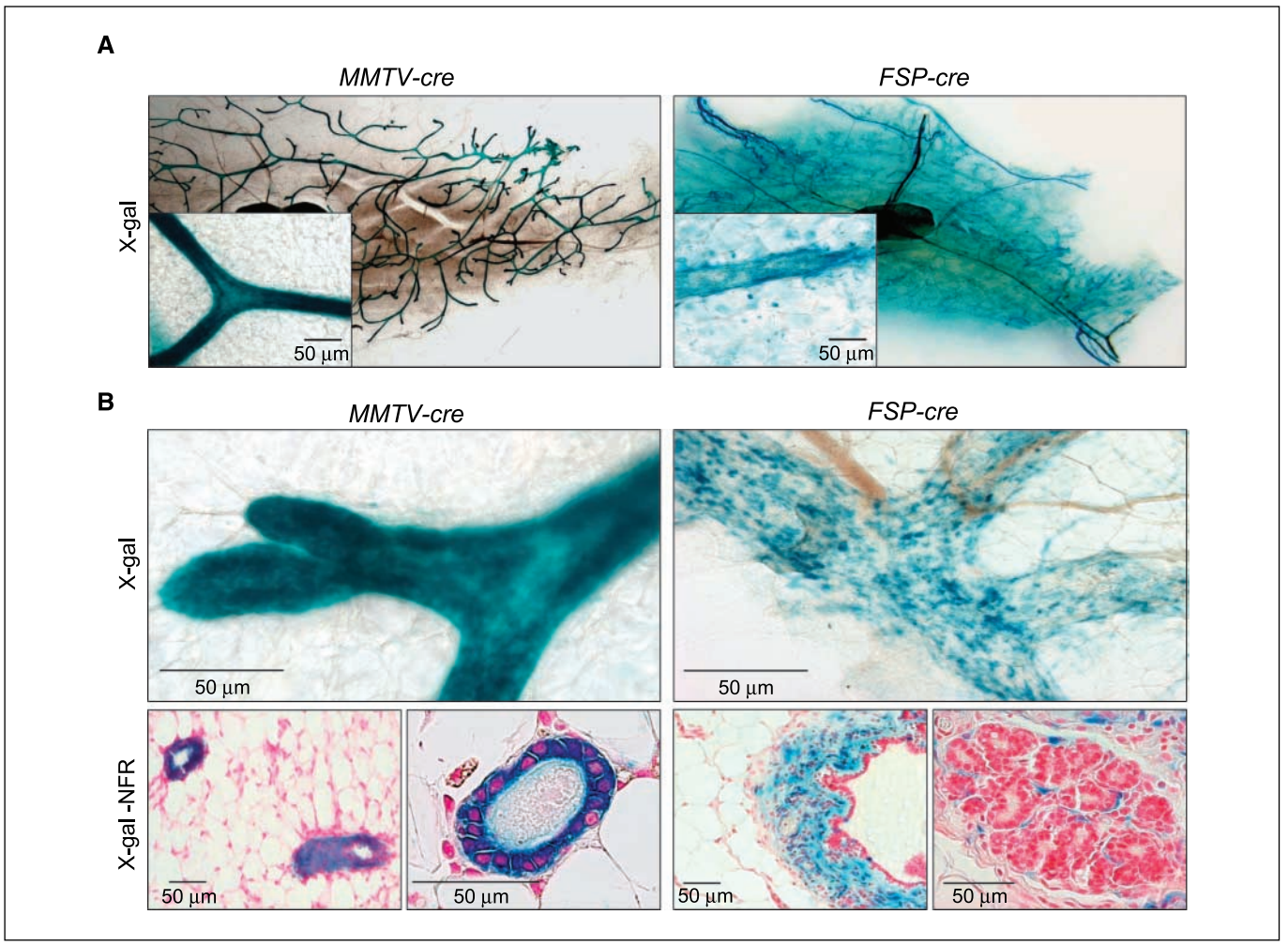

Figure 1. Analysis of epithelial and stromal *cre* expression in the mouse mammary gland. Mammary tissue obtained from virgin *MMTV-cre;Rosa*^{loxP} or *FSP-cre;Rosa*^{loxP} mice were attached to glass slides and stained for β-galactosidase activity *in situ*. Images of the glands were acquired with a handheld digital camera, whereas the mammary duct structures (*insets*) were captured by digital microscopy using the same gland (*A*). Higher magnification of whole mount tissues and stained histologic sections from other glands vividly illustrate the different staining patterns for *MMTV-cre* and *FSP-cre* mammary tissue (*B*). For better visualization, β-galactosidase–stained tissue sections were counterstained with the nuclear specific dye, nuclear fast red.

upstream floxed stop cassette leads to the induction of *LacZ* expression, which can be easily visualized as blue cells by histochemical staining with X-gal. Activation of the *Rosa26*^{LoxP} reporter in mammary epithelial cells was achieved by *cre* expression under the control of either the *whey acidic protein* (*WAP-cre*) or the *mouse mammary tumor virus* (*MMTV-cre*) promoters (21). Expression from the *WAP* promoter is strictly induced by pregnancy, whereas expression from the *MMTV* promoter is relatively independent of pregnancy. *Cre* expression in mammary stromal cells was driven by the *fibroblast specific protein-1* (*Fsp-1*) promoter (*FSP-cre*; ref. 22). Expression of *Fsp-1* has been associated with the early steps of EMT before the point that the characteristic morphologic changes take place (23). Because the expression of *Fsp-1* is an early event during EMT, we reasoned that *FSP-cre* mice could represent an effective tool to rigorously monitor the initiation of EMT *in vivo*. X-gal staining of mammary glands revealed the expected epithelial-specific expression of *cre* in virgin *MMTV-cre* (Fig. 1; blue-stained tissue) and pregnant *WAP-cre* mice (Supplementary Fig. S1). In contrast, the expression of *cre* in *FSP-cre* mice was observed in the majority of stromal cells surrounding the epithelial ducts of the mammary gland (Fig. 1*A* and *B*). Cross sections of X-gal–stained glands from *FSP-cre* mice revealed blue cells that had the characteristic morphology of adipocytes and fibroblasts (Fig. 1*B*). Cell-specific marker analysis for epithelial (cytokeratin 8/18) and mesenchymal (vimentin) cells showed that expression of *cre* in pregnant *WAP-cre* mice was restricted to cytokeratin-positive epithelial cells (Fig. 2*A*). Conversely, the expression of *cre* in virgin and pregnant mammary glands of *FSP-cre* mice was restricted to vimentin-positive cells, with no detectable expression in cytokeratin-positive cells (Fig. 2*B* and *C*). The generation and characterization of the temporal and tissue-specific expression of *cre* in this *FSP-cre* mouse model will be presented elsewhere.[8]

EMT occurs in *myc*-initiated tumors. We used these *WAP-cre* and *FSP-cre* transgenes to label epithelial and stromal cells in the mammary gland to assess the occurrence and frequency of EMT in

[8] Trimboli et al., in preparation.

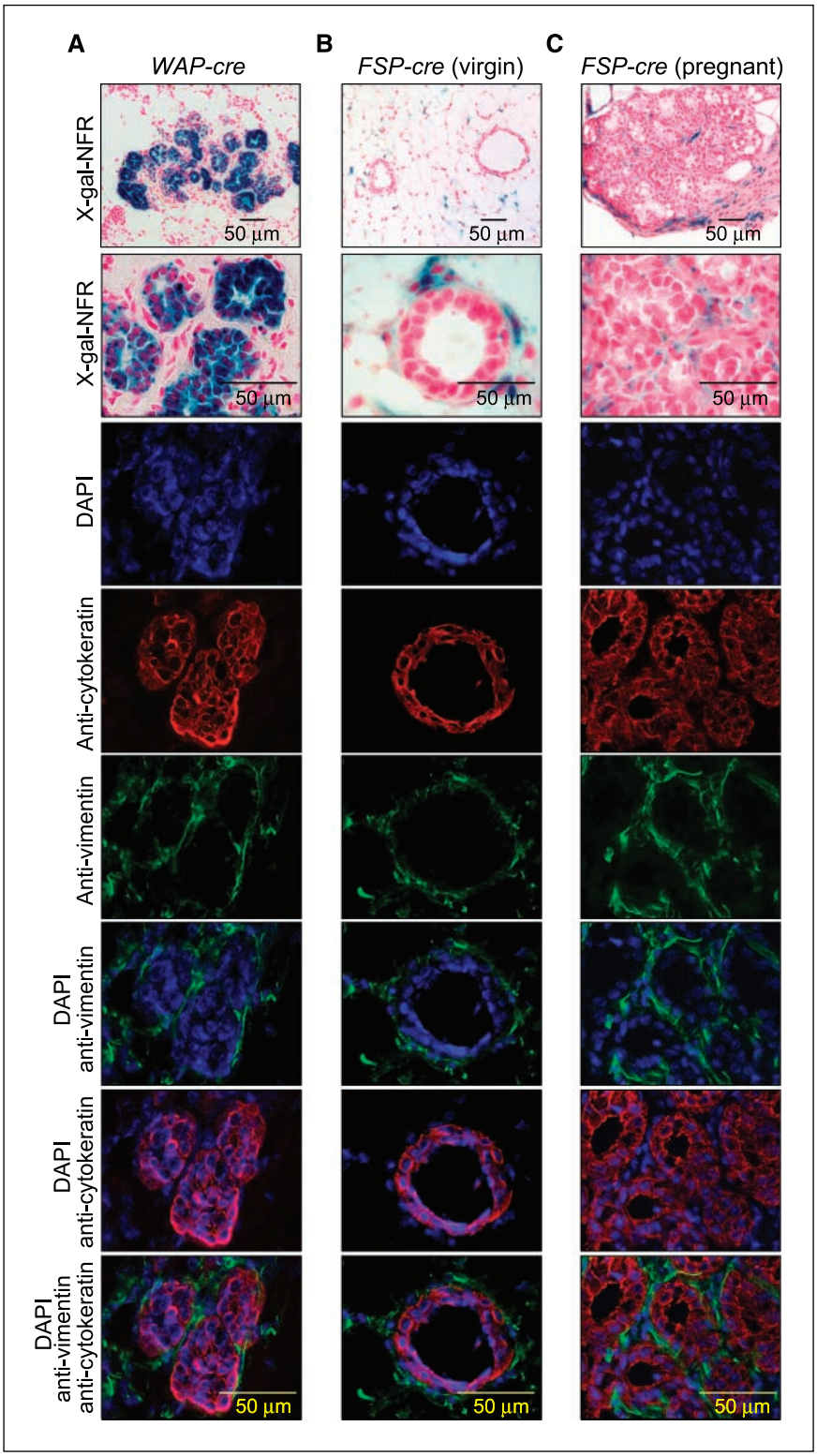

Figure 2. β-Galactosidase and immunofluorescence staining of frozen mammary tissue sections. To determine the cellular location of the *cre* transgenes using the LacZ marker, β-galactosidase activity was visualized by X-gal staining (blue precipitate) and nuclear fast red dye counterstaining. Identification of cell types was determined with antibodies to vimentin (*green*; mesenchymal) and cytokeratin 8/18 (*red*; epithelial) to carry out immunofluorescence staining on a consecutive frozen section counterstained with the nuclear fluorescent dye DAPI. The tissues shown are pregnant mammary gland from a *WAP-cre; Rosa26^{loxP}* mouse (*A*) and nonpregnant (*B*) and pregnant mammary glands from *FSP-cre; Rosa26^{loxP}* mice (*C*).

three mouse models of breast cancer: *WAP-myc* (24), *MMTV-neu* (25), and *MMTV-polyoma middle T antigen* (*MMTV-PyMT*; ref. 26). Although not representative of all known genetic abnormalities in breast cancer, these three models have unique molecular, cellular, and clinical features that can be used to evaluate different aspects of this heterogeneous disease. In *neu*-initiated mammary tumors, cells are uniformly undifferentiated with small nuclei, fine chromatin, and abundant *eosinophilic cytoplasm* (27). These cells form solid tumors with little stroma that are locally invasive in the absence of myoepithelial cells and squamous metaplasia. The *PyMT* tumors tend to have more stroma, with some glandular differentiation or cyst formation (28). In contrast, *myc*-induced

tumors contain larger cells with pleomorphic nuclei, coarse chromatin, and amphophilic cytoplasm. Importantly, these tumors are glandular in nature and have abundant stromal cells that surround the invasive tumors. Triple transgenic female mice possessing one of the three oncogenes, *WAP-cre* or *FSP-cre*, and the *Rosa26*^{LoxP} reporter were generated by appropriate interbreeding. Tumor-bearing females were harvested when the largest tumor was 2 cm in diameter. The frequency of EMT in each of the mammary tumor models was initially evaluated by the expression of *WAP-cre* in the tumor stroma and by expression of *FSP-cre* in the tumor epithelium. Epithelium- and stroma-specific expression was subsequently confirmed by immunofluorescent staining with epithelial- and mesenchymal-specific antibodies.

When *WAP-cre* was used to mark epithelial tumor cells, approximately half of the *WAP-myc* tumors stained positive for X-gal, indicative of the characteristic heterogenous pattern of expression from the *WAP-cre* transgene (ref. 21; data not shown). Strikingly, more than half of *myc*-initiated tumors contained considerable amounts of stromal tissue that stained blue (Fig. 3*A*; Supplementary Fig. S2*A* and *B*). In each case, the X-gal–positive stroma was located immediately adjacent to the tumor site and extended at least five cell layers deep. Histologic analysis of H&E sections revealed that the X-gal–positive cells had the characteristic morphologic features of mesenchymal tissue, including spindle-shaped cells with elongated nuclei and undefined cell borders, which were indistinguishable from other X-gal–negative

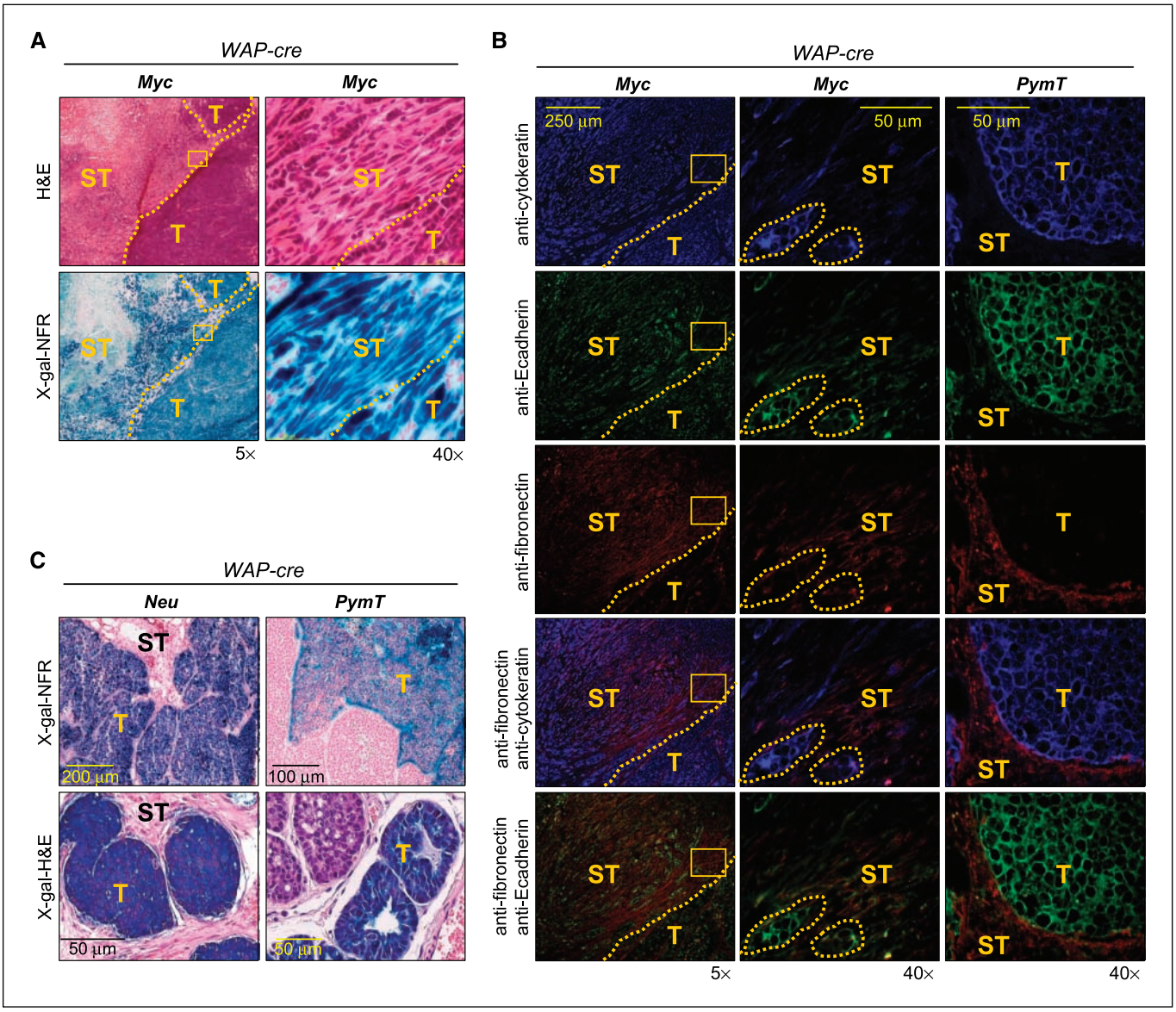

Figure 3. Immunofluorescent staining for cellular markers in EMT and non-EMT tumors. Frozen sections from *WAP-cre;WAP-myc;Rosa26*^{loxP}–labeled tumors were stained with X-gal. Note the blue staining in the stromal (*ST*) compartment surrounding the tumor (*T*); the stroma-tumor boundary is demarcated by the dotted-yellow line (*A*). Frozen mammary tumor sections from *WAP-myc* (*myc*) and *MMTV-PyMT* (*PymT*) mice were stained with two epithelial-specific markers, cytokeratin 8/18 (*blue*) and E-cadherin (*green*), and with a mesenchymal-specific marker, fibronectin (*red*; *B*). The left column contains low-magnification images from the *WAP-myc* tumor; the stroma-tumor boundary is demarcated by the dotted-yellow line. The center column contains higher-magnification images from the region in the left column outlined by the yellow rectangle. X-gal staining of tumors from the *MMTV-neu* (*neu*) and *MMTV-PyMT* (*PymT*) models (*C*).

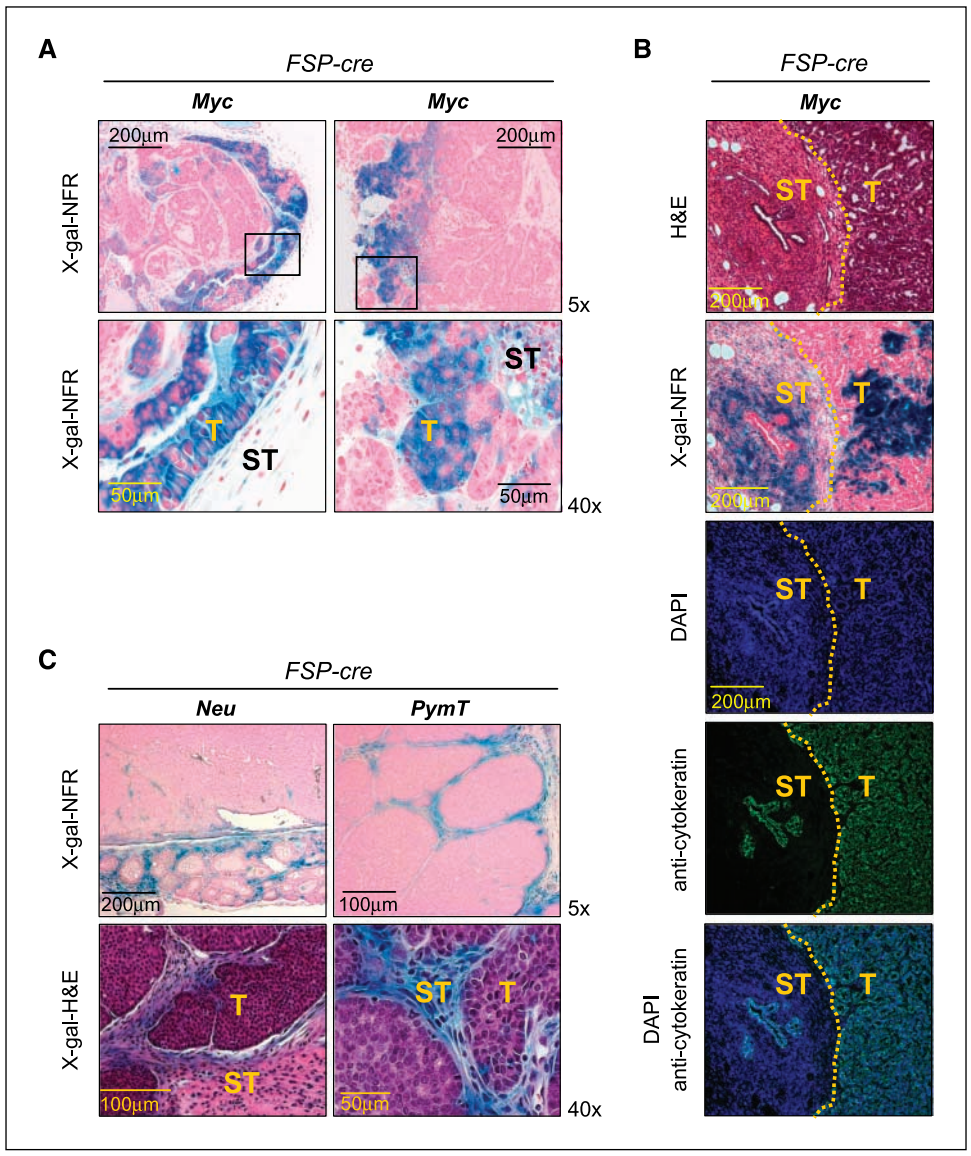

Figure 4. Evidence of early EMT in *WAP-myc* tumors. X-gal–stained sections of mammary tumors derived from *WAP-myc*;*FSP-cre;Rosa*^{loxP} mice illustrate early EMT events (blue epithelial cells); stromal (*ST*) and epithelial (*T*) compartments of tumor tissue are indicated (*A*). Consecutive frozen sections from *WAP-myc; FSP-cre;Rosa*^{loxP} tumors were stained with H&E, X-gal, or cytokeratin 8/18 (*green*) and DAPI (*blue*). Immunofluorescent staining confirms the epithelial nature of X-gal–positive (*blue*) cells within the epithelial compartment of tumors (*B*). The dotted-yellow line demarcates the tumor boundary through the series of images. X-gal–stained sections of mammary tumors derived from *MMTV-neu; FSP-cre;Rosa*^{loxP} and *MMTV-PyMT; FSP-cre;Rosa*^{loxP} models (*C*).

mesenchymal tissue in the vicinity. We then used epithelial- (cytokeratin and E-cadherin) and mesenchymal- (fibronectin) specific cell markers to confirm the identity of the X-gal–positive spindle shaped cells adjacent to the primary tumor. Immunofluorescence staining of consecutive sections revealed that some of these blue spindle-shaped cells expressed fibronectin only, whereas others expressed either fibronectin and cytokeratin or all three, fibronectin, cytokeratin, and E-cadherin (Fig. 3*B, left* and *center columns*), indicating a spectrum of late EMT stages within the same tumor microenvironment. In contrast to *WAP-myc*–initiated tumors, pathologic examination of *MMTV-neu* and *MMTV-PyMT* tumors revealed no blue cells displaying mesenchymal morphology, suggesting that late-stage EMT had not occurred in these tumor models (Fig. 3*C*; Supplementary Fig. S2*A*). Indeed, epithelial tumor cells staining positive for E-cadherin or cytokeratin 8/18 were distinctly separated from stromal cells staining positive for fibronectin (Fig. 3*C, right column*), confirming the absence of EMT in *neu*- and *PyMT*-initiated tumors.

To identify early EMT events in *myc*-initiated breast cancer, tumor-bearing *WAP-myc*;*FSP-cre;Rosa26*^{LoxP} mammary glands were analyzed by X-gal and H&E histochemical staining. As expected, the mammary gland stroma stained positive for X-gal. Importantly, distinct areas of blue staining were observed within the epithelial tumors (Fig. 4*A*). These areas contained blue cells that were cuboidal in shape and arranged into the characteristic glandular structures that form in response to *myc* overexpression (Fig. 4*A* and *B*). The X-gal–positive tumor epithelial cells retained cytokeratin and E-cadherin expression, confirming the presence of early-stage EMT in *myc*-initiated tumors (Fig. 4*B* and data not shown). Therefore, *FSP-cre* expression could identify EMT events that have not yet gone to completion. The frequency of EMT observed in tumor mice with the *FSP-cre* transgene was slightly higher than in mice with the *WAP-cre* transgene (64% versus 50%, respectively), consistent with the concept that *Fsp-1* expression is an early step in the EMT process (23). From the combined analysis of epithelial and stromal marked cells, we conclude that *myc* overexpression in mammary glands induced tumor epithelial cells to undergo the full extent of EMT.

We also evaluated tumors in *MMTV-neu;FSP-cre;Rosa26*^{LoxP} and *MMTV-PyMT;FSP-cre;Rosa26*^{LoxP} triple transgenic mice for possible

Table 1. EMT events observed for each tumor model

Tumor group	Animals	Animals with lung metastasis	Tumors with EMT/X-gal (+) tumors	%EMT
MMTV-neu + WAP-cre	14	9	0/54	0
WAP-myc + WAP-cre	9	5	11/22	50
MMTV-PyMT + WAP-cre	3	3	0/13	0
MMTV-rtTA + teto-myc	8	0	3/12	25
MMTV-neu + FSP-cre	6	3	4/78	5
WAP-myc + FSP-cre	5	3	7/11	64
MMTV-PyMT + FSP-cre	2	2	0/15	0

early signs of EMT. Pathologic analysis revealed the absence of *FSP-cre* expression in the epithelial tumor masses of these mice (Fig. 4*C*). As expected, *LacZ*-positive blue stromal cells in these tumor-bearing mammary glands were positive for vimentin and fibronectin expression and negative for both cytokeratin and E-cadherin expression (data not shown), indicating the absence of EMT in *neu*- and *PyMT*-driven tumor models. Table 1 lists the number of tumors surveyed for the four breast cancer models. This analysis indicates that EMT is a common event observed in *myc*-initiated tumors but is rarely found in *neu*- and *PyMT*-initiated mammary tumors.

One difference between these three tumor models is that *myc* expression is driven by the pregnancy-inducible *WAP* promoter whereas *neu* and *PyMT* expression is driven by the *MMTV* promoter. This difference raised concern that the EMT observed in the *WAP-myc* model could be, in part, due to the use of different promoters to drive oncogene expression. We therefore turned to a doxycycline-inducible bitransgenic system developed by Chodosh and colleagues to drive the overexpression of *myc* in mammary glands of mice (29, 30). In this system, the *MMTV* promoter drives the expression of the rtTA protein (*MMTV-rtTA*), which, in the

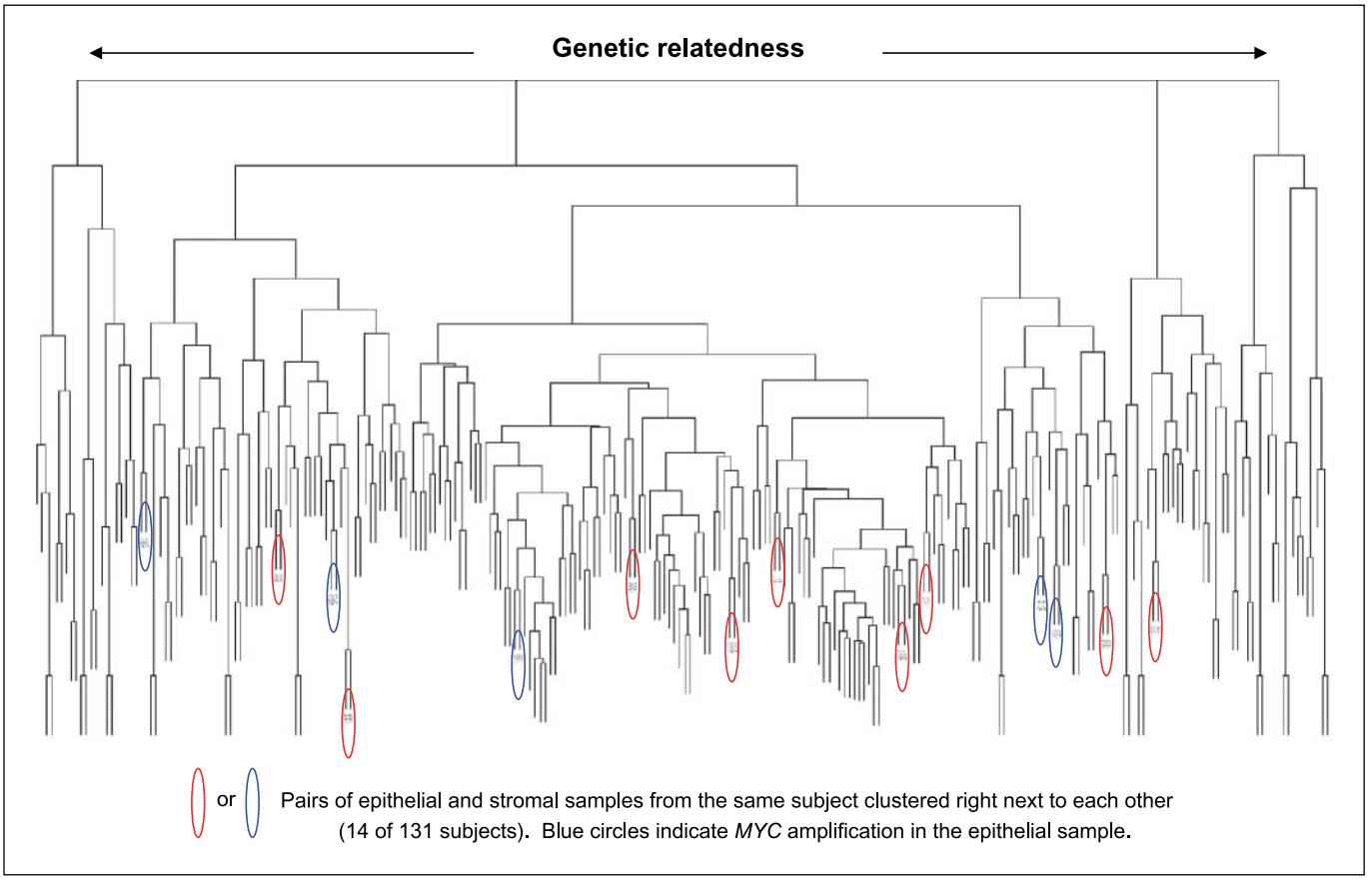

Figure 5. Hierarchical clustering of LOH data. Unsupervised hierarchical analysis was based on the occurrence of LOH or allelic imbalance (LOH/AI) at 381 informative loci from 131 stromal-epithelial paired patient tumor samples (262 total samples). LOH/AI values from each sample were compared with the entire epithelial and stromal data set. The relatedness of samples was estimated based on close LOH/AI relationships. Samples formed clusters at different levels in a hierarchical fashion, ultimately ending in pairs. These final pairings usually occurred between samples of the same cell type (not matching to a single individual; i.e., epithelium/epithelium or stromal/stromal pairings between different patients' samples). However, 14 pairs consisted of epithelium/stromal samples derived from the same patient (*red* and *blue ovals*), indicating possible occurrence of EMT in that tumor. *Blue ovals,* the five epithelial samples that were determined to contain *MYC* amplification using the polymorphic marker (D8S1128).

presence of doxycycline, binds the tet-operator and activates the expression of *myc* or *cre* (*teto-myc* and *teto-cre*). Addition of doxycycline to tetra-transgenic mice (*MMTV-rtTA;teto-myc;teto-cre;Rosa26*^{LoxP}) results in coexpression of *myc* and *cre*. These mice developed tumors that were β-galactosidase positive (Table 1 and data not shown). Of the 12 tumors analyzed, 3 tumors had morphologic features of EMT as assessed by histologic analysis of X-gal–stained sections (Supplementary Fig. S2*C*). These results show that *myc* can promote EMT irrespective of the promoter used to drive its expression.

Low frequency of EMT in invasive human breast cancer. To determine whether EMT is a common mechanism promoting the invasiveness of human cancers, we measured LOH events within the epithelial and stromal cells of invasive human breast cancers and statistically analyzed their occurrence by hierarchical clustering. Identification of an identical set of LOH events between these compartments would represent unambiguous evidence for a common cellular progenitor. Because of genomic instability in cancer, however, it is unlikely that any two cellular compartments having a common progenitor would retain an identical genetic makeup as the disease progresses. A high degree of genetic similarity between tumor epithelial and stromal cells would nonetheless indicate the likelihood of a common progenitor for these cells. Laser-captured DNA samples from the tumor epithelium and the adjacent stroma of 131 tumors were analyzed using a panel of microsatellite markers that covered all 23 chromosomes. The percentage of informative LOH reactions of a total of 381 markers was 36.7% for the epithelium, 28.4% for the stroma, and 32.6% combined, indicating that epithelial samples display higher frequencies of LOH on a per marker basis. Hierarchical cluster analysis of data from all 262 epithelial and stromal samples (131 tumors) was done based on the frequency of concordance of LOH across markers. This analysis depicted in the histogram (Fig. 5) revealed that only 14 epithelial-stromal pairs (indicated using red and blue ovals) of the 131 tumors (10.7%) clustered immediately together, indicating that tumor-associated stromal cells originate infrequently from epithelial tumor cells. Thus, our observations in human patients and animal models indicate that EMT is rare in breast cancer. A comparable study that evaluated nuclear polymorphisms between tumor epithelial and stromal cell populations also suggested that stromal cells did not frequently originate from an epithelial cell lineage (31).

The observation that EMT occurred in ~25% to 50% of *myc*-driven tumors in mice prompted us to assess the status of *MYC* using the adjacent polymorphic marker (D8S1128) in the 131 patient samples analyzed for genome-wide LOH. Of the 14 epithelial-stromal pairs that clustered immediately together, 5 had an allelic imbalance (marked with *blue ovals*, Fig. 5) for the D8S1128 marker in the epithelial sample and all of the imbalances were determined to represent amplification events (5 of 5 or 100%). On examination of the remaining 117 tumor epithelial samples, we found that 42 had imbalances present at the D8S1128 marker; 20 of these represented amplification events (20 of 42 or 48%) and the remaining represented LOH. These results suggest that *MYC* amplification is associated with the occurrence of EMT in human breast cancer [100% versus 48%; $P = 0.05$, epithelium only (Fisher's exact test)]. Indicating the possibility that whereas *myc* amplification could predispose the epithelium to undergo EMT, clearly, additional genetic insults are most likely involved in this process.

Discussion

Generation of a genetic system to mark mammary epithelial and stromal cells *in vivo*. EMT has been postulated as a mechanism by which tumor cells can acquire an invasive phenotype (32). Yet most of the evidence for the existence of EMT in cancer is derived from *in vitro* experimental systems using cancer cell lines. Direct *in vivo* evidence for EMT in cancer is lacking. Here, we developed two complementary systems to genetically manipulate the genome of stromal and mammary epithelial cells of mice. By genetically marking mammary epithelial and stromal cells and following their fate as tumors develop *in vivo*, we provide direct evidence for EMT events in cancer. In addition, these results begin to define the genetic components contributing toward EMT by showing that the *myc* oncogene, and not *neu* or *PyMT*, has the ability to induce EMT in breast cancer.

Evidence for EMT in breast cancer. The *FSP-cre* mouse model described here can be used to target the ablation of genes in the stromal compartment of mammary glands *in vivo*, and thus can provide a means to discriminate between gene function in stromal and epithelial compartments during breast cancer progression. We used the *FSP-cre* and *WAP-cre* mouse models to genetically and permanently activate expression of the *LacZ* reporter gene from the *Rosa*^{LoxP} locus in stromal and epithelial cell compartments of the mammary gland, respectively. Two sets of observations from the use of these systems have led us to conclude that *myc* can induce EMT during mammary tumorigenesis. First, by introducing the *WAP-cre* model into three established models of breast cancer, we tracked the fate of epithelial marked cells during mammary tumorigenesis. From these studies, we could unambiguously determine that stromal fibroblasts associated with *myc*-induced tumors were of epithelial origin. Many of these cells lacked cytokeratin and E-cadherin expression and instead expressed the mesenchymal-specific makers of vimentin and fibronectin. Second, introduction of *FSP-cre* into the same tumor models confirmed these results and illustrated the clonal nature of early EMT events induced by *myc*. In these cases, detection of early EMT events was characterized by *FSP-cre* transgene expression in patches of cells that were imbedded in tumor masses coexpressing epithelial-specific genes. The fact that *FSP-cre* and *WAP-cre* are never expressed in normal epithelial and fibroblast cells, respectively, has led us to conclude that these two sets of observations are a manifestation of EMT in cancer.

EMT is specifically associated with *myc*-initiated tumors. Several lines of evidence presented here suggest that EMT in breast cancer can be specifically facilitated by the *myc* oncogene. *Myc* overexpression, whether driven from the *WAP* or *MMTV* promoters, resulted in mammary tumors that typically had an abundance of adjacent stromal fibroblasts. In many cases, these fibroblasts could be shown to originate from the tumor epithelial cells. Overexpression of *neu* or *PyMT* also resulted in mammary tumors, but these had little stromal contribution and the small amount of stroma present lacked any evidence of EMT. Consistent with morphologic differences among these mouse tumor models, *myc*-derived tumors have a global expression profile that is distinct from that of *neu* and *PyMT* tumors (33). Analysis of 131 patient samples also suggests the occurrence of EMT in human breast cancer. Clustering analysis of genome-wide LOH analysis on invasive human breast cancer patient DNA samples revealed that only 14 of the 131 epithelial and stromal samples were similar to each other, indicating that EMT occurs but is infrequent. Further evaluation of

this data using the polymorphic marker (D8S1128), which resides near the *MYC* locus, established that those 14 samples were twice as likely to have *MYC* amplification compared with the 117 remaining samples, supporting an association of *MYC* with EMT.

Our data also suggest that *myc* overexpression is not sufficient for EMT to occur because only ~50% of the 45 *myc*-initiated tumors analyzed had evidence of EMT. In other words, *myc* overexpression does not necessarily lead to EMT. Moreover, early events of EMT observed in *myc*-initiated tumors expressing the *FSP-cre;Rosa1*^{LoxP} reporter were visualized as discrete clonal patches of cells within epithelial tumor masses. As discussed above, 5 of 14 human breast cancer samples had allelic imbalance (amplification) for the D8S1128 marker residing next to the *MYC* locus. These mouse and human data would suggest that additional genetic or epigenetic events are likely required to collaborate with *myc* for the full manifestation of EMT. These could include the alteration of components that function downstream or in parallel to MYC signaling. It will be important in the future to identify the select cadre of genomic alterations (genetic or epigenetic) that collaborate with *myc* and contribute to EMT in cancer, and to elucidate their mechanism of action in this process.

EMT is not a prerequisite for invasiveness and metastasis in breast cancer. The observation that EMT is specifically detected in *myc*-initiated tumors in mice and is associated with amplification of *MYC* in human patients is consistent with the highly invasive nature of these types of tumors. However, these data also suggest that EMT is not required for metastatic progression because tumors analyzed in mice and humans lacking EMT clearly had metastatic potential. Indeed, half of the mice bearing *myc*-initiated tumors and essentially all mice bearing *neu*- and *PyMT*-initiated tumors lacked any evidence of EMT, and yet many of these animals had significant amounts of lung metastases (data not shown).

Although not a prerequisite for invasive behavior, EMT may nonetheless represent one mechanism to facilitate progression toward a more aggressive metastatic cancer. In addition, the occurrence of EMT may affect other aspects of cancer biology. For example, EMT might provide tumor cells with the ability to adapt to physiologically relevant stresses such as low oxygen or nutrient levels. EMT might also have a profound consequence in the responsiveness of tumors to various therapeutic treatments. Thus, our data support the hypothesis that genetic alterations in the epithelium initiate tumorigenesis and that EMT could contribute to the microenvironment and modulate interpatient biological behavior (34).

Acknowledgments

Received 6/8/2007; revised 10/8/2007; accepted 11/12/2007.

Grant support: NIH grant P01 CA097189 (M.C. Ostrowski), Department of Defense grant BC030892 (A. de Bruin), and The Pew Charitable Trusts grant 2590SC. C. Eng is a recipient of the Doris Duke Distinguished Clinical Scientist Award, and G. Leone is the recipient of The Pew Charitable Trusts Scholar Award and the Leukemia & Lymphoma Society Scholar Award.

The costs of publication of this article were defrayed in part by the payment of page charges. This article must therefore be hereby marked *advertisement* in accordance with 18 U.S.C. Section 1734 solely to indicate this fact.

References

1. Bates RC, DeLeo, MJ, Mercurio AM. The epithelial-mesenchymal transition of colon carcinoma involves expression of IL-8 and CXCR-1-mediated chemotaxis. Exp Cell Res 2004;299:315–24.
2. Bakin AV, Tomlinson AK, Bhowmick NA, Moses HL, Arteaga CL. Phosphatidylinositol 3-kinase function is required for transforming growth factor β mediated epithelial to mesenchymal transition and cell migration. J Biol Chem 2000;275:36803–10.
3. Oft M, Heider KH, Beug H. TGFβ signaling is necessary for carcinoma cell invasiveness and metastasis. Curr Biol 1999;8:1243–52.
4. Thiery JP. Epithelial-mesenchymal transitions in development and pathologies. Curr Opin Cell Biol 2003;15:740–6.
5. Thiery JP. Epithelial-mesenchymal transitions in tumour progression. Nat Rev Cancer 2002;2:442–54.
6. Huber MA, Kraut N, Beug, H. Molecular requirements for epithelial-mesenchymal transition during tumor progression. Curr Opin Cell Biol 2005;17:548–58.
7. Xue C, Plieth D, Venkov C, Xu C, Neilson EG. The gatekeeper effect of epithelial-mesenchymal transition regulates the frequency of breast cancer metastasis. Cancer Res 2003;63:3386–94.
8. Mikaelian I, Blades N, Churchill GA, et al. Proteotypic classification of spontaneous and transgenic mammary neoplasms. Breast Cancer Res 2004;6:R668–79.
9. Moody SE, Perez D, Pan TC, et al. The transcriptional repressor Snail promotes mammary tumor recurrence. Cancer Cell 2005;8:197–209.
10. Tarin D. The fallacy of epithelial mesenchymal transition in neoplasia. Cancer Res 2005;65:5996–6000.
11. Thompson EW, Newgreen DF. Carcinoma invasion and metastasis: a role for epithelial-mesenchymal transition? Cancer Res 2005;65:5991–5.
12. Soriano P. Generalized lacZ expression with the ROSA26 Cre reporter strain. Nat Genet 1999;21:70–1.
13. Strutz F, Okada H, Lo CW, et al. Identification and characterization of a fibroblast marker: FSP1. J Cell Biol 1995;130:393–405.
14. Okada H, Danoff TM, Fischer A, Lopez-Guisa JM, Strutz F, Neilson EG. Identification of a novel *cis*-acting element for fibroblast-specific transcription of the FSP1 gene. Am J Physiol 1998;275:F306–14.
15. Gu H, Zou YR, Rajewsky K. Independent control of immunoglobulin switch recombination at individual switch regions evidenced through Cre-loxP-mediated gene targeting. Cell 1993;73:1155–64.
16. Overbeek PA, Aguilar-Cordova E, Hanten G, et al. Coinjection strategy for visual identification of transgenic mice. Transgenic Res 1991;1:31–7.
17. Taketo M, Schroeder AC, Mobraaten LE, et al. FVB/N: an inbred mouse strain preferable for transgenic analyses. Proc Natl Acad Sci U S A 1991;88:2065–9.
18. Kurose K, Hoshaw-Woodard S, Adeyinka A, Lemeshow S, Watson PH, Eng C. Genetic model of multi-step breast carcinogenesis involving the epithelium and stroma: clues to tumour-microenvironment interactions. Hum Mol Genet 2001;10:1907–13.
19. Kurose K, Gilley K, Matsumoto S, Watson PH, Zhou XP, Eng C. Frequent somatic mutations in PTEN and TP53 are mutually exclusive in the stroma of breast carcinomas. Nat Genet 2002;32:355–7.
20. Eisen MB, et al. Cluster analysis and display of genome-wide expression patterns. Proc Natl Acad Sci U S A 1998;95:14863–8.
21. Wagner KU, Wall RJ, St-Onge L, et al. Cre-mediated gene deletion in the mammary gland. Nucleic Acids Res 1997;25:4323–30.
22. Bhowmick NA, Chytil A, Plieth D, et al. TGF-β signaling in fibroblasts modulates the oncogenic potential of adjacent epithelia. Science 2004;303:848–51.
23. Okada H, Danoff TM, Kalluri R, Neilson EG. Early role of Fsp1 in epithelial-mesenchymal transformation. Am J Physiol 1997;273:F563–74.
24. Schoenenberger CA, Andres AC, Groner B, van der Valk M, LeMeur M, Gerlinger P. Targeted c-myc gene expression in mammary glands of transgenic mice induces mammary tumours with constitutive milk protein gene transcription. EMBO J 1988;7:169–75.
25. Guy CT, Webster MA, Schaller M, Parsons TJ, Cardiff RD, Muller WJ. Expression of the neu protooncogene in the mammary epithelium of transgenic mice induces metastatic disease. Proc Natl Acad Sci U S A 1992;89:10578–82.
26. Guy CT, Cardiff RD, Muller WJ. Induction of mammary tumors by expression of polyomavirus middle T oncogene: a transgenic mouse model for metastatic disease. Mol Cell Biol 1992;12:954–61.
27. Cardiff RD, Anver MR, Gusterson BA, et al. The mammary pathology of genetically engineered mice: the consensus report and recommendations from the Annapolis meeting. Oncogene 2000;19:968–88.
28. Rosner A, Miyoshi K, Landesman-Bollag E, et al. Pathway pathology: histological differences between ErbB/Ras and Wnt pathway transgenic mammary tumors. Am J Pathol 2002;161:1087–97.
29. D'Cruz CM, Gunther EJ, Boxer RB, et al. c-MYC induces mammary tumorigenesis by means of a preferred pathway involving spontaneous Kras2 mutations. Nat Med 2001;7:235–9.
30. Gunther EJ, Belka GK, Wertheim GB, et al. A novel doxycycline-inducible system for the transgenic analysis of mammary gland biology. FASEB J 2002;16:283–92.
31. Allinen M, Beroukhim R, Cai L, et al. Molecular characterization of the tumor microenvironment in breast cancer. Cancer Cell 2004;6:17–32.
32. Vincent-Salomon A, Thiery JP. Host microenvironment in breast cancer development: epithelial-mesenchymal transition in breast cancer development. Breast Cancer Res 2003;5:101–6.
33. Desai KV, Xiao N, Wang W, et al. Initiating oncogenic event determines gene-expression patterns of human breast cancer models. Proc Natl Acad Sci U S A 2002;99:6967–72.
34. Fukino K, Shen L, Matsumoto S, Morrison CD, Mutter G, Eng C. Combined total genome loss of heterozygosity scan of breast cancer stroma and epithelium reveals multiplicity of stromal targets. Cancer Res 2004;64:7231–6.